

## Research Article

# Mathematical Modeling of Transient Responses in a Large Scale Multiconductor System

**Caiwang Sheng and Xiaoqing Zhang**

*National Active Distribution Network Technology Research Center, School of Electrical Engineering, Beijing Jiaotong University, Beijing 100044, China*

Correspondence should be addressed to Caiwang Sheng; shengcaiwang@msn.cn

Received 5 June 2014; Revised 13 July 2014; Accepted 15 July 2014; Published 5 August 2014

Academic Editor: Michael Chen

Copyright © 2014 C. Sheng and X. Zhang. This is an open access article distributed under the Creative Commons Attribution License, which permits unrestricted use, distribution, and reproduction in any medium, provided the original work is properly cited.

This paper proposes a reduced-order model for the large scale circuits representing the multiconductor systems. It is based on the block Arnoldi algorithm for calculating congruence transformation matrix. By setting up the state equations in frequency domain for the multiconductor systems, the transfer functions are calculated and so the frequency response curves are obtained. A comparison is made between those curves obtained from the circuits with and without reduced-order treatment and a better agreement appears between them. By using inverse Laplace transform, the lightning transient responses in the multiconductor systems are given in time-domain. A better agreement is shown between calculated and experimental results, which confirm the validity of the proposed model.

## 1. Introduction

An external lightning protection system of a structure is usually constituted by numerous interconnected longitudinal and transverse conducting branches. It takes a form of three-dimensional multiconductor system and can be converted into an equivalent passive RLC network. For an actual tall structure, its external lightning protection system is large in physical dimension and complex in construction, which results in a large scale equivalent network. From the view point of lightning protection design, the need exists for obtaining lightning transient responses of the equivalent network. For the sake of saving storage capacity and computation time, a simplification should be made for the equivalent network; otherwise the circuit calculation is difficult to perform. From the existing research on lightning transient responses [1–6], we have almost not found the relevant procedure that can give a great simplification for the large scale equivalent network. Therefore, the order reduction model is necessary for the transient analysis of lightning protection systems. Recently, the investigation on passive network synthesis has been reported in literature [7–10], which is closely related

to the order reduction model. The investigation work is of practical significance in analysis of large scale electrical networks. Based on the achievement of the existing work, a reduced-order algorithm (ROA) is introduced in this paper as a Krylov space method which provides a passive, stable, and accurate macromodel compared with the reduction techniques [11, 12]. In order to reduce the matrices directly in the system state equation, the transformation matrix can be calculated by using the block Arnoldi algorithm [13]. In the ROA, we have developed a robust framework by unveiling the connections between the passive reduction technique and other well known Krylov space based processes. In terms of the reduced-order model of the structure under study, amplitude-frequency and phase-frequency curves can be quantitatively calculated and so we can compare those curves with the frequency response curves of the original circuit system. Furthermore, the time function can be obtained with the help of the inverse Laplace transform and the lightning transient response is given by using the convolution theorem. The comparison is also made between calculated and measured results to confirm the validity of the proposed model.

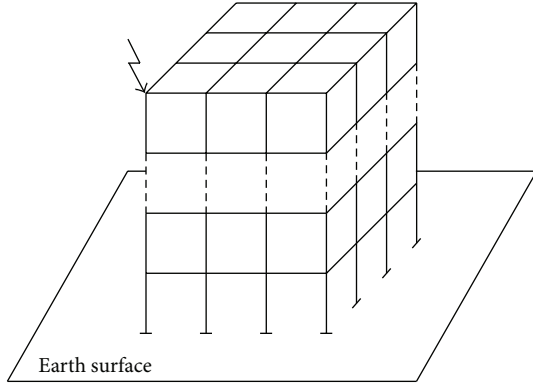


FIGURE 1: A cage-like multiconductor system.

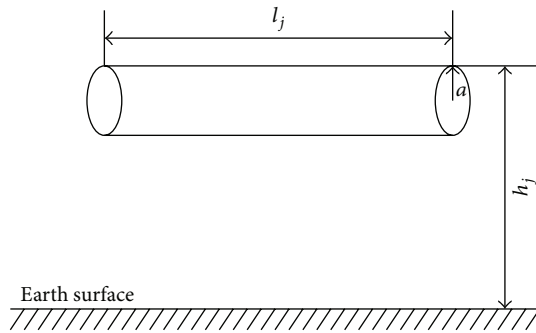


FIGURE 2: A horizontal conducting branch.

## 2. State Equations of the Equivalent Circuit

Figure 1 shows the configuration of a cage-like multiconductor system formed by vertical and horizontal conducting branches. For setting up the state equations of the equivalent network, the electrical parameters of the conducting branches in the multiconductor system are represented by resistances, inductances, and capacitances. Since the distance between the two conducting branches is much greater than their respective radius, the electromagnetic couplings between them can be ignored. Therefore, the formulas for evaluating the electrical parameters are derived as follows.

Consider a horizontal conducting branch in the multiconductor system, as shown in Figure 2. Its capacitance can be expressed by [14]

$$C_j = \frac{2\pi\epsilon_0 l_j}{\ln(2h_j/a) - D_1}, \quad (1)$$

where  $D_1 = \ln\left(1 + \sqrt{1 + (4h_j^2/l_j^2)}\right) + (2h_j/l_j) - \sqrt{1 + (4h_j^2/l_j^2)} + 0.307$ .

Similarly, the capacitance of a vertical conducting branch, as shown in Figure 3, can be expressed by [14]

$$C_k = \frac{2\pi\epsilon_0 l_k}{\ln(l_k/a) - D_2}, \quad (2)$$

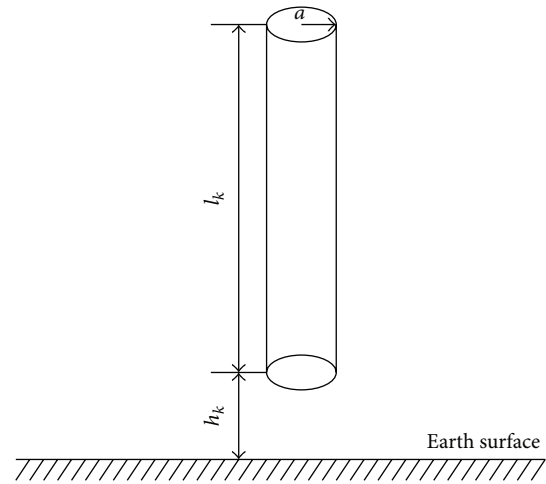


FIGURE 3: A vertical conducting branch.

where the coefficient  $D_2$  is

$$D_2 = \begin{cases} 1 + \frac{h_k}{l_k} \ln \frac{4h_k}{l_k} + \left(1 + \frac{h_k}{l_k}\right) \ln \left(1 - \frac{h_k}{l_k}\right) \\ - \left(1 + \frac{2h_k}{l_k}\right) \ln \left(1 + \frac{2h_k}{l_k}\right) & \frac{h_k}{l_k} < 1, \\ 0.307 + \left(1 + \frac{h_k}{l_k}\right) \ln \left(1 + \frac{l_k}{h_k}\right) \\ - \left(1 + \frac{2h_k}{l_k}\right) \ln \left(1 + \frac{l_k}{2h_k}\right) & \frac{h_k}{l_k} > 1. \end{cases} \quad (3)$$

According to the electromagnetic analogy [15], the product of capacitance and inductance is equal to that of space permeability  $\mu_0$  and permittivity  $\epsilon_0$ . This gives the inductances for horizontal and vertical conducting branches

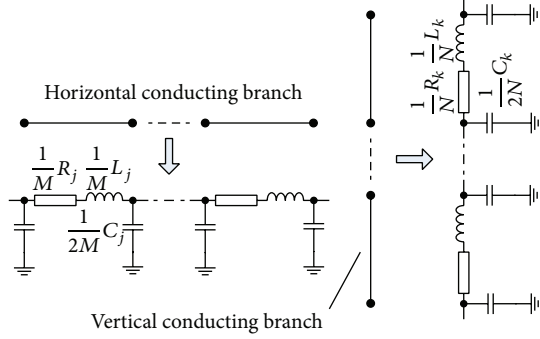
$$\begin{aligned} L_j &= \frac{\mu_0 \epsilon_0}{C_j}, \\ L_k &= \frac{\mu_0 \epsilon_0}{C_k}. \end{aligned} \quad (4)$$

Additionally, the conductance of an arbitrary conducting branch is estimated by

$$G_\xi = \frac{1}{\rho} \cdot \frac{\pi a^2}{l_\xi}, \quad (5)$$

where  $\rho$  is the resistivity of conducting branch and the subscript  $\xi$  takes as  $j$  or  $k$ .

In consideration of the propagation phenomenon of lightning current, each conducting branch of the multiconductor system is subdivided into a suitable number of segments. The length of each segment is assumed to be less than or equal to one-tenth of the wavelength corresponding to the maximum frequency likely to affect the system transient [16]. Each segment is represented by a  $\pi$ -type circuit, as shown

FIGURE 4: A  $\pi$ -type circuit of a two-segment subsystem.

in Figure 4, where  $M$  and  $N$  are the segment numbers of horizontal and vertical branches, respectively.

As a result, the multiconductor system is converted into an equivalent network constituting a large number of  $\pi$ -type circuits. On the basis of the electrical parameters calculated from (1)–(5), the capacitance, conductance, and inductance matrices can be formed for the equivalent network:

$$\begin{aligned} \mathbf{C} &= \text{diag} [C_1, C_2, \dots, C_{n_C}], \\ \mathbf{G} &= \text{diag} [G_1, G_2, \dots, G_{n_G}], \\ \mathbf{L} &= \text{diag} [L_1, L_2, \dots, L_{n_L}], \end{aligned} \quad (6)$$

where the subscripts  $n_C$ ,  $n_G$ , and  $n_L$  denote the total numbers of capacitances, conductances, and inductances of the equivalent network, respectively. The circuit components of the equivalent network are numbered in the sequence of capacitances, inductances, and lightning current source. In accordance with the component number, the incidence matrix of the equivalent network is written as

$$\mathbf{A} = [\mathbf{A}_C, \mathbf{A}_L, \mathbf{A}_S]. \quad (7)$$

The node voltages (i.e., the voltages across the capacitances) and the currents through the inductances are selected as the state variables:

$$\mathbf{x} = [u_{n_1}, u_{n_2}, \dots, u_{n_\beta}, i_{L_1}, i_{L_2}, \dots, i_{L_{n_L}}]^T, \quad (8)$$

where the subscript  $\beta$  denotes the total node number of the equivalent network. Thus, the state equation is set up for the equivalent network:

$$\begin{aligned} \mathbf{P}\dot{\mathbf{x}} + \mathbf{Q}\mathbf{x} &= \mathbf{B}i_s(t), \\ u_o(t) &= \mathbf{B}^T \mathbf{x}, \end{aligned} \quad (9)$$

where

$$\begin{aligned} \mathbf{P} &= \begin{bmatrix} \widehat{\mathbf{C}} & \mathbf{0} \\ \mathbf{0} & \mathbf{L} \end{bmatrix}, \\ \mathbf{Q} &= \begin{bmatrix} \widehat{\mathbf{G}} & \mathbf{A}_L \\ -\mathbf{A}_L^T & \mathbf{0} \end{bmatrix}, \\ \mathbf{B} &= \begin{bmatrix} \mathbf{A}_S \\ \mathbf{0} \end{bmatrix}, \end{aligned} \quad (10)$$

where  $\widehat{\mathbf{C}} = \mathbf{A}_C \mathbf{C} \mathbf{A}_C^T$  and  $\widehat{\mathbf{G}} = \mathbf{A}_L \mathbf{G} \mathbf{A}_L^T \in \mathfrak{R}^{\beta \times \beta}$ . Note that  $\widehat{\mathbf{C}}$ ,  $\mathbf{L}$ , and  $\widehat{\mathbf{G}}$  are symmetric and nondefinite matrices.

Next, the so-called transfer function can be calculated, which describes the input-output behavior of a linear dynamical system (9) in frequency domain [17]. Taking the Laplace transformation of (9), the transfer function is given by

$$\mathbf{H}(s) = \mathbf{B}^T (\mathbf{Q} + s\mathbf{P})^{-1} \mathbf{B}. \quad (11)$$

The computation of  $\mathbf{H}(s)$  is called simulation in frequency domain and of course not done by calculating  $(\mathbf{Q} + s\mathbf{P})^{-1}$ . However, it is still expensive for large system. For this reason, the reduced-order model is necessarily proposed in this paper.

### 3. Reduced-Order Model

For simplifying the lightning transient calculation of the large scale RLC network, the ROA is employed here. The algorithm is based on the block Arnoldi method. Therefore, we introduce our notion of block Krylov subspaces for multiple starting vectors.

**3.1. Model Order Reduction Techniques.** A widely used class of model order reduction techniques is the class of Krylov subspace methods. Before block Krylov subspace methods are used, the two matrices  $\mathbf{Q}$  and  $\mathbf{P}$  in (11) have to be reduced, denoted by  $\mathbf{D}$  in the following. This can be done by rewriting (11) as

$$\mathbf{H}(s) = \mathbf{B}^T (\mathbf{I} + s\mathbf{D})^{-1} \mathbf{W}, \quad (12)$$

where

$$\begin{aligned} \mathbf{D} &= \mathbf{Q}^{-1} \mathbf{P}, \\ \mathbf{W} &= \mathbf{Q}^{-1} \mathbf{B}. \end{aligned} \quad (13)$$

Although  $\mathbf{Q}$  and  $\mathbf{P}$  are sparse matrices, in general, the matrix  $\mathbf{D}$  is a dense matrix. However, block Krylov subspace methods involve  $\mathbf{D}$  only in the form of matrix-vector products  $\mathbf{D}\mathbf{w}$  and possibly  $\mathbf{D}^T \mathbf{w}$  [18].

The proper definition of block Krylov subspaces is necessary to be involved and the use of these subspaces results in much more efficient reduced-order modeling techniques. The block Krylov space generated by matrices  $\mathbf{D} \in \mathfrak{R}^{(\beta+n_L) \times (\beta+n_L)}$  and  $\mathbf{W} = [\mathbf{w}_1 \ \mathbf{w}_2 \ \dots \ \mathbf{w}_\zeta] \in \mathfrak{R}^{(\beta+n_L) \times \zeta}$  is defined as

$$\text{Kr}(\mathbf{D}, \mathbf{W}, q) = \text{colsp} [\mathbf{W}, \mathbf{D}\mathbf{W}, \mathbf{D}^2\mathbf{W}, \dots, \mathbf{D}^q\mathbf{W}]. \quad (14)$$

**3.2. The Algorithm of Calculating Congruence Transformation Matrix.** The congruence transformation matrix  $\mathbf{V}$  is calculated based on the above definition of  $\text{Kr}(\mathbf{D}, \mathbf{W}, q)$ . Here,  $\mathbf{V} = [\mathbf{v}_1 \ \mathbf{v}_2 \ \dots \ \mathbf{v}_q] \in \mathfrak{R}^{(\beta+n_L) \times q}$  is an orthonormal matrix and subjected to  $\mathbf{V}^T \mathbf{V} = \mathbf{I}$  ( $\mathbf{I} \in \mathfrak{R}^{q \times q}$  is an identity matrix) [19]. The classical Arnoldi process [20] generates orthonormal basis vectors for the sequence of Krylov subspaces  $\text{Kr}(\mathbf{D}, \mathbf{W}, q)$ ,  $q \geq 1$ , induced by  $\mathbf{D}$  and  $\mathbf{W}$ . In order

to saving storage capacity and computation time, a smaller value of the order  $q$  is better. In fact, exact deflation at step  $q$  of the Arnoldi-type process occurs if and only if  $\tilde{\mathbf{v}}_q = \mathbf{0}$ . Similarly, inexact deflation occurs if and only if  $\|\tilde{\mathbf{v}}_q\| \approx 0$ , but  $\tilde{\mathbf{v}}_q \neq \mathbf{0}$ . Therefore, the order  $q$  will be determined according to  $\|\tilde{\mathbf{v}}_q\| \leq \text{dtol}$ , where  $\text{dtol} \geq 0$  is a suitably chosen deflation tolerance. A simple Arnoldi-type algorithm is presented in the following [18].

- (0) Set  $\tilde{\mathbf{v}}_i = \mathbf{w}_i$  ( $i = 1, 2, \dots, m$ ).  
Set  $m_c = m$ .  
For  $n = 1, 2, \dots, k$  do the following:
  - (1) compute  $\|\tilde{\mathbf{v}}_q\|$  and check if the deflation criterion ( $\|\tilde{\mathbf{v}}_q\| \leq \text{dtol}$ ) is fulfilled.  
If yes,  $\tilde{\mathbf{v}}_q$  is deflated by doing the following.  
Set  $m_c = m_c - 1$ . If  $m_c = 0$ , set  $q = q - 1$  and stop.  
Set  $\tilde{\mathbf{v}}_i = \tilde{\mathbf{v}}_{i+1}$  for  $i = q, q + 1, \dots, q + m_c - 1$ .  
Return to step (1).
  - (2) Set  $h_{q,q-m_c} = \|\tilde{\mathbf{v}}_q\|$  and  $\mathbf{v}_q = \tilde{\mathbf{v}}_q/h_{q,q-m_c}$ .
  - (3) Compute  $\mathbf{v}_{q+m_c} = \mathbf{D}\mathbf{v}_q$ .
  - (4) For  $i = 1, 2, \dots, q$  do the following:  
set  $h_{i,q} = \mathbf{v}_i^T \tilde{\mathbf{v}}_{q+m_c}$  and  $\tilde{\mathbf{v}}_{q+m_c} = \tilde{\mathbf{v}}_{q+m_c} - \mathbf{v}_i h_{i,q}$ .
  - (5) For  $i = q-m_c+1, q-m_c+2, \dots, q-1$  do the following:  
set  $h_{q,i} = \mathbf{v}_q^T \tilde{\mathbf{v}}_{i+m_c}$  and  $\tilde{\mathbf{v}}_{i+m_c} = \tilde{\mathbf{v}}_{i+m_c} - \mathbf{v}_q h_{q,i}$ .

**3.3. A Reduced-Order Algorithm.** After computing the transformation matrix  $\mathbf{V}$ , we can easily find the ROA matrices. Applying the change of variable  $\mathbf{x} = \mathbf{V}\tilde{\mathbf{x}}$  in (9) and multiplying both sides by  $\mathbf{V}^T$  give

$$\begin{aligned} (\mathbf{V}^T \mathbf{P} \mathbf{V}) \dot{\tilde{\mathbf{x}}} + (\mathbf{V}^T \mathbf{Q} \mathbf{V}) \tilde{\mathbf{x}} &= (\mathbf{V}^T \mathbf{B}) i_s(t) \\ u_o(t) &= (\mathbf{B}^T \mathbf{V}) \tilde{\mathbf{x}}. \end{aligned} \quad (15)$$

For the macromodel, the reduced-order matrices are

$$\begin{aligned} \tilde{\mathbf{P}} &= \mathbf{V}^T \mathbf{P} \mathbf{V}, \\ \tilde{\mathbf{Q}} &= \mathbf{V}^T \mathbf{Q} \mathbf{V}, \\ \tilde{\mathbf{B}} &= \mathbf{V}^T \mathbf{B}. \end{aligned} \quad (16)$$

These types of transformations are known as congruence transformations. From (15) and (16), the reduced-order transfer function is given by

$$\tilde{\mathbf{H}}(s) = \tilde{\mathbf{B}}^T (\tilde{\mathbf{Q}} + s\tilde{\mathbf{P}})^{-1} \tilde{\mathbf{B}}. \quad (17)$$

Define

$$\begin{aligned} \tilde{\mathbf{D}} &= \tilde{\mathbf{Q}}^{-1} \tilde{\mathbf{P}}, \\ \tilde{\mathbf{W}} &= \tilde{\mathbf{Q}}^{-1} \tilde{\mathbf{B}}. \end{aligned} \quad (18)$$

The reduced system can be formulated as

$$\begin{aligned} \tilde{\mathbf{D}} \dot{\tilde{\mathbf{x}}} + \tilde{\mathbf{x}} &= \tilde{\mathbf{W}} i_s(t) \\ u_o(t) &= \tilde{\mathbf{B}}^T \tilde{\mathbf{x}}. \end{aligned} \quad (19)$$

By applying any eigendecomposition routine on  $\tilde{\mathbf{D}}$ , we can obtain

$$\tilde{\mathbf{D}} = \mathbf{J} \mathbf{\Lambda} \mathbf{J}^{-1}, \quad (20)$$

where  $\mathbf{\Lambda}$  is a diagonal matrix. Since  $\tilde{\mathbf{D}}$  is a real matrix, any complex eigenvalue or eigenvector has its conjugate. Therefore, we can use real  $\mathbf{J}$  and  $\mathbf{\Lambda}$  matrices in the following transformations:

$$\begin{aligned} \mathbf{J}_r &= \mathbf{J} \mathbf{K}^{-1}, \\ \mathbf{\Lambda}_r &= \mathbf{K} \mathbf{\Lambda} \mathbf{K}^{-1}, \end{aligned} \quad (21)$$

where

$$\tilde{\mathbf{D}} = \mathbf{J}_r \mathbf{\Lambda}_r \mathbf{J}_r^{-1}, \quad (22)$$

and  $\mathbf{J}_r, \mathbf{\Lambda}_r \in \mathfrak{R}^{q \times q}$ .  $\mathbf{K} \in \mathbb{C}^{q \times q}$  is the transformation matrix that can be defined as follows:

$$\begin{aligned} \text{if } \Lambda_{i,i} \text{ is real, } K_{i,i} &= 1; \\ \text{if } \Lambda_{i,i} &= \bar{\Lambda}_{i+1,i+1}, \begin{bmatrix} K_{i,i} & K_{i,i+1} \\ K_{i+1,i} & K_{i+1,i+1} \end{bmatrix} = \begin{bmatrix} 1 & 1 \\ j & -j \end{bmatrix}. \end{aligned}$$

$\mathbf{\Lambda}_r$  will contain  $2 \times 2$  blocks on the diagonal for complex eigenvalues, and  $1 \times 1$  blocks for the real eigenvalues. By substituting (22) into (19), we can get

$$\begin{aligned} (\mathbf{J}_r \mathbf{\Lambda}_r \mathbf{J}_r^{-1}) \dot{\tilde{\mathbf{x}}} + \tilde{\mathbf{x}} &= \tilde{\mathbf{W}} i_s(t), \\ u_o(t) &= \tilde{\mathbf{B}}^T \tilde{\mathbf{x}}. \end{aligned} \quad (23)$$

The final transfer function is given by

$$\tilde{\mathbf{H}}(s) = \tilde{\mathbf{B}}^T \mathbf{J}_r^{-1} (\mathbf{\Lambda}_r^{-1} s + \mathbf{I}_q)^{-1} \mathbf{J}_r \tilde{\mathbf{W}}. \quad (24)$$

As a result, we can obtain the final reduced-order model in the following form:

$$\begin{aligned} \tilde{H}_{ij}(s) &= \sum_{m=1}^q \frac{\tilde{K}_{(ij)m}}{(s + \tilde{p}_m)} + d \\ &= \frac{b_{ijk} s^q + \dots + b_{ij1} s + b_{ij0}}{s^q + a_{k-1} s^{q-1} + \dots + a_1 s + a_0}, \end{aligned} \quad (25)$$

where  $\tilde{H}_{ij}(s) = \tilde{H}_{ji}(s)$ ,  $1 \leq i, j \leq N$ ,  $\tilde{p}$  and  $\tilde{K}$  are the dominant pole and corresponding residue, respectively,  $q$  is the number of reduce-order, and  $d$  represents any direct coupling between ports.

#### 4. Time-Domain Simulation of the Reduced-Order Model

For a complete simulation of circuit response, the linear elements should be simulated along with the reduced-order macromodels. Here, we describe a method to include the ROA macromodel. The method is based on a  $y$ -parameter description of the macromodel [21]. In order to calculate the  $y$ -parameters of the reduced-order system, the eigendecomposition steps [(22) and (24)] are used. After obtaining the final form of the transfer function  $\tilde{H}_{ij}(s)$ , the time function  $\tilde{h}_{ij}(t)$  can be calculated by using inverse Laplace transform of partial fraction expansion.

According to (25), we need to transform the rational fraction into proper fraction. So, we can get the following:

$$\tilde{H}_{ij}(s) = d + \frac{\tilde{y}_{ij}(s)}{u_{ij}(s)}, \quad (26)$$

where the remainder term  $\tilde{y}_{ij}(s)/u_{ij}(s)$  is a proper fraction.

The denominator polynomials can be factored via partial fraction expansion, and the roots of the equation  $u_{ij}(s) = 0$  are solved. The roots of the equations have two kinds of situation, such as simple root and conjugate complex.

(i) If the equation  $u(s) = 0$  has  $n$  simple roots, we can set the  $n$  simple roots as  $p_1, p_2, \dots, p_n$ . Therefore, the expansion form of  $\tilde{H}(s)$  is

$$\tilde{H}(s) = \frac{K_1}{s-p_1} + \frac{K_2}{s-p_2} + \dots + \frac{K_n}{s-p_n}, \quad (27)$$

where  $K_i = \tilde{y}(s)/u'(s)|_{s=p_i}$ ,  $i = 1, 2, 3, \dots, n$ .

After determining the coefficients of (27), the time function is

$$h(t) = \sum_{i=1}^n \frac{\tilde{y}(s)}{u'(s)} e^{p_i t}. \quad (28)$$

(ii) If the equation  $u(s) = 0$  has two conjugate complex roots ( $p_1 = \alpha + j\omega$ ,  $p_2 = \alpha - j\omega$ ), we thus have

$$K_1 = \left[ (s - \alpha - j\omega) \tilde{H}(s) \right]_{s=\alpha+j\omega} = \left. \frac{\tilde{y}(s)}{u'(s)} \right|_{s=\alpha+j\omega}, \quad (29)$$

$$K_2 = \left[ (s - \alpha + j\omega) \tilde{H}(s) \right]_{s=\alpha-j\omega} = \left. \frac{\tilde{y}(s)}{u'(s)} \right|_{s=\alpha-j\omega}.$$

We set  $K_1 = |K_1| e^{j\theta_1}$  and  $K_2 = |K_1| e^{-j\theta_1}$ ; thus

$$\begin{aligned} h(t) &= K_1 e^{(\alpha+j\omega)t} + K_2 e^{(\alpha-j\omega)t} \\ &= |K_1| e^{j\theta_1} e^{(\alpha+j\omega)t} + |K_1| e^{-j\theta_1} e^{(\alpha-j\omega)t} \\ &= 2 |K_1| e^{\alpha t} \cos(\omega t + \theta_1). \end{aligned} \quad (30)$$

Subsequent to the calculation of the time function  $h_{ij}(t)$ , convolution is needed for time-domain analysis. Hence, the circuit response in time-domain at the ports can be given by

$$y_{ij}(t) = \sum_{j=1}^N \int_0^t u_j(t) h_{ij}(t-\tau) d\tau, \quad 1 \leq i \leq n, \quad (31)$$

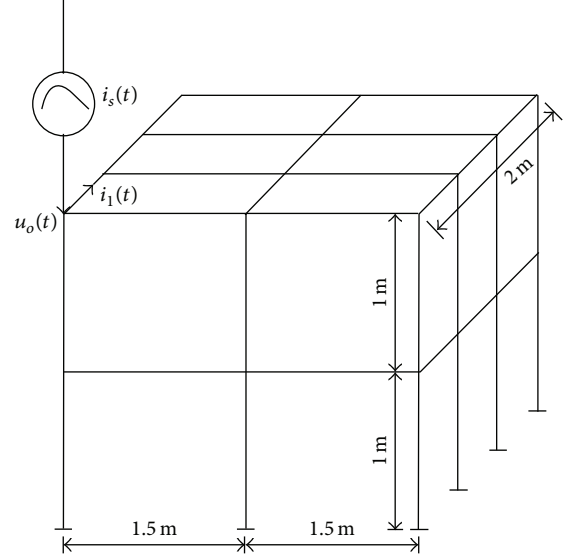


FIGURE 5: The structure diagram of a reduced-scale model.

TABLE 1: The dimension of the matrices and the computational time for the original and reduced model.

System	Order	Computational time (s)
Original	69	5.680
ROA	10	1.779

which requires  $O(T^2)$  complexity, where  $T$  is the number of time points during simulation. For this reason, recursive convolution [22] and time-domain  $y$ -parameter macromodels [21] were developed, where the complexity is linear with the number of time points. The algorithms of these approaches are used by MATLAB in detail.

#### 5. Numerical Example

A reduced-scale structure of lightning protection system is shown in Figure 5. The diameter of each steel bar is 8 mm. According to the above model and algorithm, the programs are written by MATLAB. Table 1 summarizes the reduction results of matrix dimension and the computational time by using ROA.

In order to verify the validity of the reduced-order model proposed above, the amplitude-frequency curves and phase-frequency curves of original and reduced-order model are computed, as shown in Figures 6 and 7.

From the two figures above, we can see that a better agreement appears between original and reduced-order model.

For the sake of computing the circuit response of the reduced-scale model, the injection lightning current needs to be known. The waveform of the current source  $i_s(t)$  is shown in Figure 8. Therefore, the circuit response of reduced-order model is computed by the program we have written. The waveforms of the lightning transient responses  $i_1(t)$  and  $u_o(t)$  can be obtained and they are compared with that measured experimentally [23] as shown in Figures 9 and 10. It can be

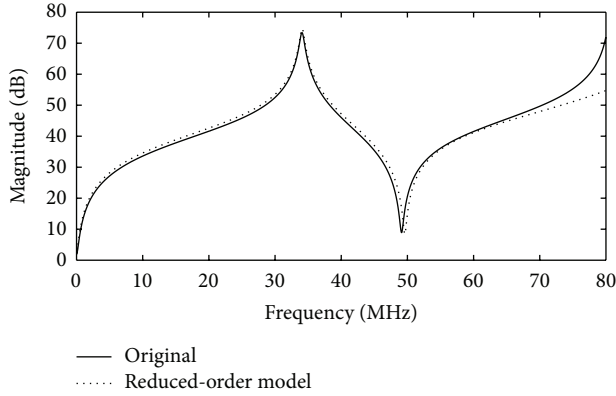


FIGURE 6: The amplitude-frequency curves of the circuit.

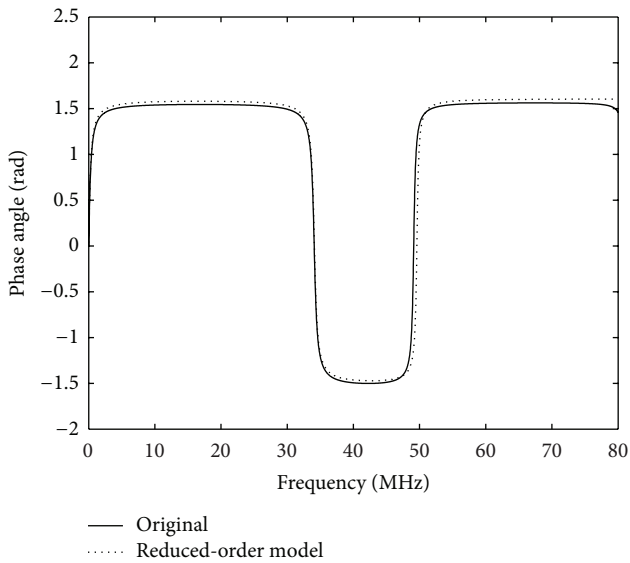


FIGURE 7: The phase-frequency curves of the circuit.

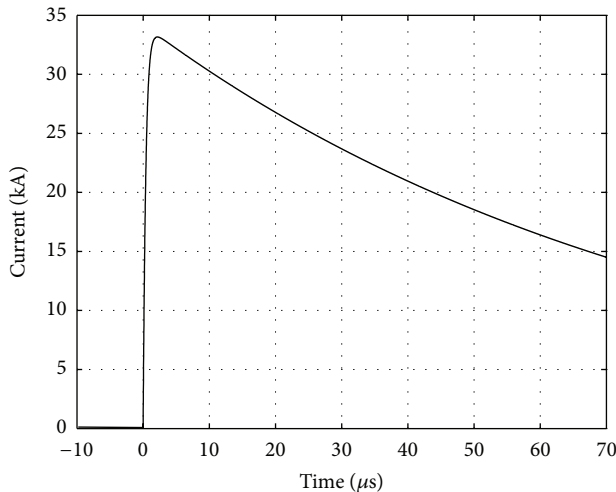


FIGURE 8: The waveform of injection current.

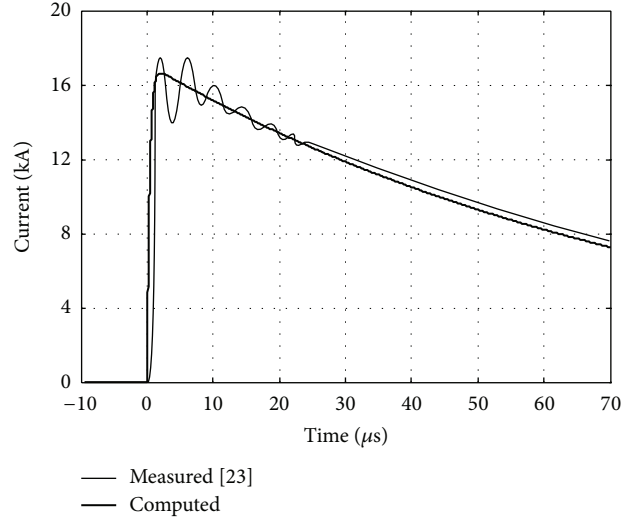


FIGURE 9: Measured and computed current response curves for the reduced-scale structure.

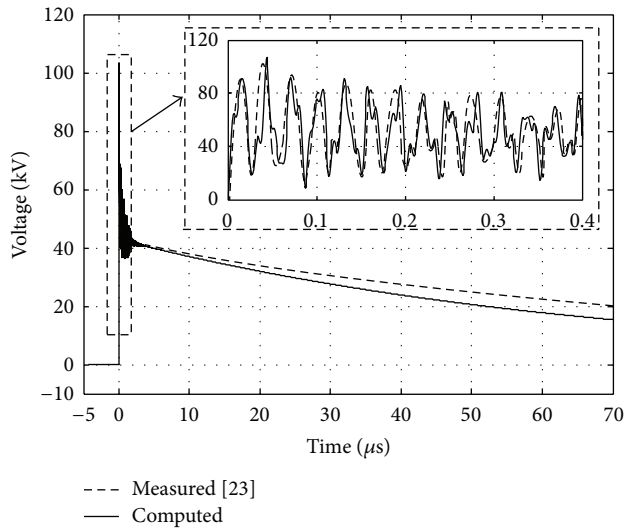


FIGURE 10: Measured and computed voltage response curves for the reduced-scale structure.

seen from Figures 8 and 9 that very good agreement is also found between computed and measured results.

## 6. Conclusions

A novel reduced-order macromodeling algorithm has been proposed for calculating the lightning transient responses in the lightning protection systems of structures. The reduced-order model given here uses the block Arnoldi algorithm to reduce the matrix dimension. On the basis of matrix operation and discretization, the amplitude-frequency curves and phase-frequency curves can be obtained by means of the MATLAB program. These curves under including and excluding the reduced-order treatment are compared with each other and a better agreement is shown between them. The inverse Laplace transform of partial fraction expansion

has also been performed for time-domain analysis. The computed lightning transient responses in a lightning protection system conform reasonably with those from experimental measurement, which confirms the validity of the proposed model.

### Conflict of Interests

The authors declare that there is no conflict of interests regarding the publication of this paper.

### Acknowledgment

This work was financially supported by the National Natural Science Foundation of China under Contract no. 50977002.

### References

- [1] K. J. Kerns, I. L. Wemple, and A. T. Yang, "Stable and efficient reduction of substrate model networks using congruence transforms," in *Proceedings of the 1995 IEEE/ACM International Conference on Computer-Aided Design (ICCAD '95)*, pp. 207–214, November 1995.
- [2] L. T. Pillage and R. A. Rohrer, "Asymptotic waveform evaluation for timing analysis," *IEEE Transactions on Computer-Aided Design of Integrated Circuits and Systems*, vol. 9, no. 4, pp. 352–366, 1990.
- [3] P. Feldmann and R. W. Freund, "Efficient linear circuit analysis by Pade approximation via the Lanczos process," *IEEE Transactions on Computer-Aided Design of Integrated Circuits and Systems*, vol. 14, no. 5, pp. 639–649, 1995.
- [4] L. M. Silveira, M. Kamon, and J. White, "Efficient reduced-order modeling of frequency-dependent coupling inductances associated with 3-D interconnect structures," in *Proceedings of the 32nd Design Automation Conference (DAC '95)*, pp. 376–380, June 1995.
- [5] E. J. Grimme, *Krylov projection methods for model reduction [Ph.D. dissertation]*, University of Illinois at Urbana-Champaign, Champaign, Ill, USA, 1997.
- [6] D. L. Boley, "Krylov space methods on state-space control models," *Circuits, Systems, and Signal Processing*, vol. 13, no. 6, pp. 733–758, 1994.
- [7] M. Z. Q. Chen, K. Wang, M. Yin, C. Li et al., "Synthesis of n-port resistive networks containing 2n terminals," *Int. J. Circ. Theor. Appl.*, 2013.
- [8] K. Wang, M. Z. Q. Chen, and Y. Hu, "Synthesis of biquadratic impedances with at most four passive elements," *Journal of the Franklin Institute*, vol. 351, pp. 1251–1267, 2014.
- [9] M. Z. Q. Chen, K. Wang, Z. Shu, and C. Li, "Realizations of a special class of admittances with strictly lower complexity than canonical forms," *IEEE Transactions on Circuits and Systems. I. Regular Papers*, vol. 60, no. 9, pp. 2465–2473, 2013.
- [10] M. Z. Q. Chen, K. Wang, Y. Zou, and J. Lam, "Realization of a special class of admittances with one damper and one inerter for mechanical control," *IEEE Transactions on Automatic Control*, vol. 58, no. 7, pp. 1841–1846, 2013.
- [11] A. Odabasioglu, M. Celik, and L. T. Pileggi, "PRIMA: passive reduced-order interconnect macromodeling algorithm," *IEEE Transactions on Computer-Aided Design of Integrated Circuits and Systems*, vol. 17, no. 8, pp. 645–654, 1998.
- [12] A. Odabasioglu, M. Celik, and L. T. Pileggi, "Practical considerations for passive reduction of RLC circuits," in *Proceedings of the 1999 IEEE/ACM International Conference on Computer-Aided Design (ICCAD '99)*, pp. 214–219, November 1999.
- [13] R. W. Freund, "Reduced-order modeling techniques based on Krylov subspaces and their use in circuit simulation," in *Applied and Computational Control, Signals, and Circuits, Vol. 1*, Appl. Comput. Control Signals Circuits, pp. 435–498, Birkhäuser, Boston, Mass, USA, 1999.
- [14] U. Y. Yosseli, E. S. Kochanov, and M. G. Stryncki, *Calculation of Capacitances*, Energy Press, Moscow, Russian, 1981.
- [15] C. Z. Feng, *Electromagnetic Field Theory*, Higher Education Press, Beijing, China, 2002.
- [16] S. Cristina and A. Orlandi, "Calculation of the induced effects due to a lightning stroke," *IEE Proceedings B*, vol. 139, no. 4, pp. 374–380, 1992.
- [17] M. Günther, M. Hoschek, and P. Rentrop, "Differential-algebraic equations in electric circuit simulation," *International Journal of Electronics and Communications*, vol. 57, pp. 101–107, 2000.
- [18] R. W. Freund, "Krylov-subspace methods for reduced-order modeling in circuit simulation," *Journal of Computational and Applied Mathematics*, vol. 123, no. 1-2, pp. 395–421, 2000.
- [19] K. J. Kerns and A. T. Yang, "Stable and efficient reduction of large, multiport RC networks by pole analysis via congruence transformations," *IEEE Transactions on Computer-Aided Design of Integrated Circuits and Systems*, vol. 16, no. 7, pp. 734–744, 1997.
- [20] W. E. Arnoldi, "The principle of minimized iteration in the solution of the matrix eigenvalue problem," *Quarterly of Applied Mathematics*, vol. 9, pp. 17–29, 1951.
- [21] S. Y. Kim, N. Gopal, and L. T. Pillage, "Time-domain macromodels for VLSI interconnect analysis," *IEEE Transactions on Computer-Aided Design of Integrated Circuits and Systems*, vol. 13, no. 10, pp. 1257–1270, 1994.
- [22] V. Raghavan, J. E. Bracken, and R. A. Rohrer, "AWESpice: a general tool for the accurate and efficient simulation of interconnect problems," in *Proceedings of the 29th ACM/IEEE Design Automation Conference*, pp. 87–92, June 1992.
- [23] I. A. Metwally, F. H. Heidler, and W. J. Zischank, "Magnetic fields and loop voltages inside reduced- and full-scale structures produced by direct lightning strikes," *IEEE Transactions on Electromagnetic Compatibility*, vol. 48, no. 2, pp. 414–426, 2006.